Analysis of the thermal performances of uninsulated and bio-based insulated compressed earth blocks walls: from the material to the wall scale

Giada Giuffrida, Laurent Ibos, Abderrahim Boudenne, Hamza Allam

Analysis of the thermal performances of uninsulated and bio-based insulated compressed earth blocks walls: from the material to the wall scale

Giada Giuffrida[a*], Laurent Ibos[a], Abderrahim Boudenne[a] , Hamza Allam[a]

[a] *University of Paris Est-Creteil, Certes, Paris, France*

The lively international debate on the future of the built environment has placed the emphasis on the possibilities offered by bio and geo-based building materials. Among these, raw earth-based materials offer several advantages associated to their reusability and low embodied energy.
Nowadays, several emerging companies are basing their corporate assets on prefabricated raw earth products, as is the case of compressed earth blocks (from now on CEB). CEBs are commercialized for the construction of massive vertical envelopes, characterized by a high thermal inertia. Nevertheless, in order to compete with conventional building materials, it is also necessary to guarantee a high thermal resistance.
In this work, this issue is overcame by the design and testing of full-scale uninsulated and bio-based thermal insulated CEB walls. In this way, the thermal performance of CEB walls can be increased so to respond to the high energy requirements which are currently adopted in European Countries.
More in detail, this work reports the results of the experimental thermal and physical material characterization of the analyzed CEBs and of two innovative bio-based insulations (lime hemp and sugarcane bagasse panels), and compared them with measurements made on full-scale uninsulated and insulated CEB walls. For this purpose, walls are tested inside a double-room climatic chamber where they are subjected to variable temperatures on the two faces reproducing typical indoor and outdoor conditions during summer and winter conditions in a continental climate.
Results show the enhancement of thermal performances of compressed earth block walls when thin layers of bio-based thermal insulations are added. The thermal resistance of weakly bio-based insulated CEB walls is found to be nine times (for the sugarcane bagasse insulated CEB wall) and four times (for the lime hemp insulated CEB wall) higher than that of uninsulated CEB walls. Moreover, the addition of the insulation layers enhance the time lag and the decrement factor of compressed earth block walls.

Keywords: compressed earth blocks; lime hemp; sugarcane bagasse; material characterization; thermal performance; hot guarded box.

1. Introduction

The built environment is the hub around which human activities are concentrated; suffice it to say that in Europe people spend around 90% of their time inside buildings [1]. It is well known that Architecture, Engineering and construction (AEC) sector account for the 40% of Europe's energy consumptions, while generating the 36% of GHG emissions in the EU. Moreover, construction and demolition waste (CDW) accounts for 25%-30% of the total European waste generation.
It is thus obvious the efforts made by central authorities, AEC actors and international policies in providing a framework for rethinking the way we design, build and maintain the built environment over time. Nowadays the reduction of energy consumptions and emission of greenhouse gases is being included in various energy and environmental standards, accompanied by the need of assessing the circularity of constructions and infrastructures [2].
The challenges herein briefly reported are at the core of the intertwined green and energy transition policies promoted by the EU, and they are reflected in the three major goals identified by the *European Construction, built environment and energy efficient building Technology Platform* (ECTP). In particular, the three addressed goals are: (1) reaching clean built environment and cities, (2) built for and with the people and (3) generate prosperous construction ecosystem.
In this context, new production lines using more sustainable components and materials are being developed. Bio-based materials, waste materials and urban mining [3], with their reduced environmental impacts in the production phase, are at the core of several industries assets as it happens for *Cycle terre* company (France), whose production of earth-based products derives from the excavations of the *Grand Paris* infrastructure network.

Compressed earth blocks are building products made from a damp mix of raw earth, sand and eventually a stabilizer (cement or lime). This earth mix is then poured into steel presses and compressed either with a mechanic or a pneumatic process. The compaction of the earth mixes allows for the increase of the block density and consequently the improvement of the block's mechanical performances. As a consequence of their increased density and reorganization of their macrostructure by the compaction process, CEBs' thermal conductivity can change, as we will see in the following paragraphs. Due to their density, CEBs are endowed with high thermal inertia but poor thermal insulating properties [4, 5].

There is therefore a need to enhance the thermal performance of CEB envelopes in order to reduce heat losses in winter and heat gains in summer. To achieve these results, building envelopes with adequate inertial mass but also appropriate thermal resistance are needed. In this sense, it seems to be promising the design of CEB walls in simple, double or more complex wall configurations, as for instance cavity wall or insulated wall, in combination with insulations layers endowed with compatible vapor permeability values to CEB ones.

Several works have focused on the assessment of the thermal behavior of raw earth historical walls built in different techniques (rammed earth, adobe [4]), while few studies focused on contemporary raw earth building techniques [5], and even less on the combination of raw earth walls coupled with thermal insulations [6, 7, 8].

In absence of insulation panels [5], five different types of earth products, including proctor compacted full blocks, hypercompacted full blocks, hypercompacted full blocks with hemp fibres, hypercompacted hollow blocks and conventional fired bricks are tested at the material and at the wall scale. The bulk and dry density, the porosity and the water content of these samples are assessed. Moreover, the earth blocks and the fired bricks are equalized at three different levels of relative humidity (RH%=25%, RH%=62% and RH%=95) at a constant temperature of 23°C. Under these conditions, thermal conductivity is measured using a hot disk apparatus. For the fired bricks, thermal conductivity is around 0.75 W/mK for every RH% condition. For the hypercompacted and hemp bricks, thermal conductivity slightly varies between 1.45 W/mK and 1.55 W/mK for the firsts, and from 1.30 W/mK to 1.35 W/mK for the seconds; this change in performance is due to their low porosity. For the proctor bricks, the lower porosity allows a higher moisture storage inside the blocks, causing an increase of thermal conductivity: indeed, it ranges from 0.85 W/mK to 1.35 W/mK. At the wall scale, wall samples constituted by the same earth products are tested inside a hot guarded box (HGB) equipment, in static and dynamic conditions. Results of this study show that the fired bricks wall, despite having a lower thermal conductivity at a material scale, performs worse than the unfired earth blocks wall due to its incapacity of storing and exchanging pore water with the environment. Proctor unfired earth blocks wall performs better than hypercompacted unfired earth block wall because of its lower density and consequently, lower thermal conductivity (0.94 W/mK compared to 1.33 W/mK). The addition of hemp fibers in the hypercompacted unfired earth blocks, produces an improvement of the thermal performance at a wall scale by the 4.5% (1.27 W/mK compared to 1.33 W/mK).

In presence of insulation panels [6] two wall types were compared in two test boxes, the first one realized with a 0.29-m thick rammed earth wall and the other using the same construction system with a 0.06 m exterior layer of wood fiber insulation panel and a straw-clay render. Walls are monitored in a Csa climate. For the uninsulated rammed earth south wall is found a thermal lag between 6.5 h and 9 h (respectively for sunny and cloudy days), while for the insulated rammed earth south wall is found a thermal lag between 8.2h and 9.8h (respectively for sunny and cloudy days). Moreover, the thermal stability coefficient TSC (i.e. the ratio between outside thermal amplitude and south wall thermal amplitude) is comprised between 0.191 and 0.256 for the uninsulated rammed earth box and between 0.030 and 0.059 for the insulated rammed earth box. The authors conclude that in the case of thin rammed earth walls, the use of an external layer of thermal insulation achieve better dynamic parameters compared to uninsulated rammed earth and other conventional construction technologies [6].

Another study investigates the opportunities of combining cob earth walls with bio-based thermal insulation [7]. In particular, this work focuses on the design of two types of cob mixes: the best dense mix has a thermal conductivity of 0.45 W/mK, and the best light mix (called thermal cob and obtained by incorporating hemp shiv in the earth matrix) has a thermal conductivity of 0.12 W/mK. On the base of these material properties, the authors design a dual layer monolithic cob wall, and calculate a total thermal resistance of 3.35 m^2 K/W, i.e., U-value of 0.30 W/ m^2 K.

A similar study has been developed in [9], which tested rammed earth walls and lightweight earth panels in a heat flow meter with guarded ring. A combined wall using an interior layer of 0.03-m thick lightweight earth panels and an exterior layer of 0.12 m-thick rammed earth has an attenuation value comprised between 0.53 and 0.83 and a thermal lag comprised between 3.87 h and 4.07 h.
Another study on possible thermal insulation for raw earth walls has been proposed by [8]. In this case, adobe walls were insulated from the inside with 0.05 m-thick reed mattress realized with a cane growing spontaneously in the Andean lakes. The addition of this thin thermal insulation layer, together with other bioclimatic design strategies at the building scale, allowed keeping the indoor air temperatures always above 5°C with positive peaks at 15°C, even when outdoor temperature lies below 0°C.
This work aims at advancing the state of knowledge on the convenience of combining massive walls made of unfired earth (and in particular of compressed earth blocks) with bio-based thermal insulations. The choice fell on bio-based insulations for their renowned low embodied carbon [10, 11] and for their compatibility in terms of water vapor permeability values with earth-based materials [7, 9, 8].
The effectiveness of these types of insulations on CEB walls was evaluated in a Hot Guarded Box equipment, as done before by Bruno et al [5]. Compared to this work, the present study focuses on the difference in thermal behavior between uninsulated CEB walls, and CEB walls insulated with lime hemp panels or sugarcane bagasse panels. The walls are tested in a double climate chamber that allows to apply different temperatures on the two faces of the wall, in order to reproduce typical indoor and outdoor conditions. In this study, two types of tests were carried out on the walls: a set of static tests to determine the heat flow exchanged between indoors and outdoors under stationary conditions, resulting in the assessment of the thermal resistance of the wall in question; and a dynamic test to evaluate the inertial characteristics of the insulated and uninsulated CEB wall. Results show the interest of using natural materials for CEB façade insulation.

2. Materials and methods

2.1 Materials

Compressed earth block (CEB)

Compressed earth blocks are made by compacting damp admixtures of raw earth and aggregates in mechanical or pneumatic presses. The CEBs used in this study are realized with a mix made of 65% of raw earth (composed by clays, silts, sands and small gravels) and 35% sand (with a particle size distribution comprised between 0 and 2 mm or from 0 to 4 mm) from Paris region [12]. The environmental performance of 0.30 m thick CEB walls has been calculated by the manufacturing company *Cycle Terre* and it has been found a footprint of 27.8 kg eq CO_2 [12] for the production phase of 1 m^2 functional unit. In the literature, dry density ranging from 1600 kg/m^3 to 2760 kg/m^3 have been found [13]. In [14], the specific heat capacity of earth brick is assessed to be 869 J/kg K, whereas in [15] is found a value of 1000 J/kg K; moreover in [16], it is assessed to be equal to 808 J/kg K. Finally, thermal conductivity of CEBs seems to be strictly correlated with dry density values. Indeed, in [13, 17] thermal conductivity of CEBs range from 0.62 W/mK to 1.48 W/mK, the large dispersion of values being due to the change in dry density.

Lime hemp (LH)

Lime-hemp or hempcrete is a biomass-based product, which is currently used for non-load-bearing purposes in new construction to produce blocks for walling systems, but also for roof insulation. The use of hemp shivs and lime or cement leads to insulating mixes with low dry density (ranging from 200 kg/m^3 to 800 kg/m^3) and thermal conductivity values (ranging from 0.06 W/m K to 0.18 W/m K) [18]. Lime hemp or hempcrete materials have also high specific heat capacity, being it around 1500 J/kg K in the dry state and up to 2900 J/kg K at 99% RH [19].

Sugarcane bagasse (SB)

Sugarcane bagasse is an agricultural waste, a byproduct obtained after extraction of the juice from sugarcane stalks [20]. Various studies [20, 21] reported that its chemical composition is composed by cellulose, hemicellulose, lignin. The cellulose content of sugarcane bagasse helps to reduce the use of synthetic binders. Considering the abundance of sugarcane bagasse, it is currently investigated as an ideal raw material to produce low-cost green thermal insulation which could also satisfies environmental regulations, given its biodegradability and reusability.
Previous studies found that sugarcane bagasse insulation materials exhibited thermal conductivity ranging from 0.03 to 0.05 W/m K for densities between 100 kg/m^3 and 200 kg/m^3 [20]. Sugarcane bagasse panels used in this study were provide by *Emerwall* company.

Table 1. Material properties found in the literature

Material / Supplier	Material composition	Dry density [kg/m^3]	Specific heat capacity [J/kg K]	Thermal conductivity [W/m K]
CEB (*Cycle Terre*)	raw earth, sand [12]	1600 – 2760 [13]	869 [14] 1000 [15] 808 [16]	0.62 – 1.48 [13, 17]
Lime Hemp	Hemp shives, lime [18, 19]	200 - 800 [18]	1500 – 2900 [19]	0.06 – 0.18 [18]
Sugarcane Bagasse (*Emerwall*)	cellulose, hemicellulose, lignin [20, 21]	100 – 200 [20]	-	0.03 – 0.05 [20]

Combined walls

In this work three 0.60 x 0.60 m CEB walls have been tested. The first one is an uninsulated compressed earth wall (CEB wall) with a thicknesses of 0.15 m. The second wall, is composed by a 0.15 m thick compressed earth block wall combined with a 0.06 m-thick sugarcane bagasse panel (CEB+SB wall). The third wall is realized by juxtaposing a 0.15 m thick compressed earth block wall to a 0.06 m-thick lime hemp insulation (CEB+LH wall). The insulation layers are always applied to the outmost layer of CEB walls in order to take advantage of the thermal inertia of the CEB wall, according to what has been found in previous research [7, 22, 23]. A scheme of the tested walls is given in figure 1.

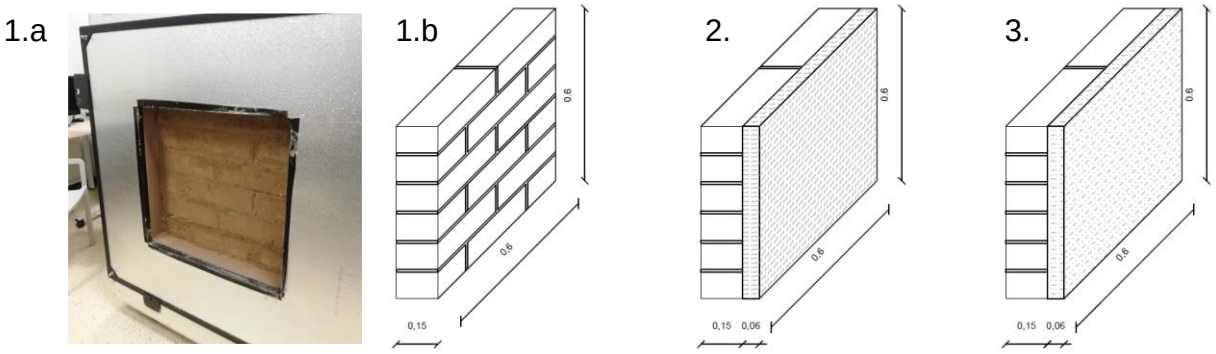

Figure 1. CEB wall (1a and 1b), sugarcane bagasse insulated CEB wall (2) and lime hemp insulated CEB wall (3)

2.2 Methods

2.2.1 Material characterization

A material characterization campaign was carried out on the three materials studied: compressed earth blocks (CEB), lime hemp (LH) and sugarcane bagasse (SB) thermal insulations. The characterization comprises the assessment of dry density, specific heat capacity and temperature dependent thermal conductivity.

Dry density of samples was assessed after oven-drying of samples at 70 °C (about 7% RH) to constant weight until steady state was reached (namely, two measures 24 hours apart differ of less than 0.1% $m_{(t,t+24)} < 0.1\%$). After oven-drying, samples were weighted and their mass divided for the volume (sizes of samples were assessed via a caliper).

Temperature dependent thermal conductivity was assessed after conditioning 0.02 m-thick CEB and 0.06 m-thick LH and SB samples in an oven, at increasing temperatures of T = 25°C, T = 30°C, T = 35°C and T = 40°C. Thermal conductivity and specific heat capacity were assessed when samples' mass was stabilized: more in detail, a condition of mass stabilization $m_{(t,\,t+24)} < 0.1\%$ was adopted because of the need of adopting bigger sizes of samples due to minimal thermal conductivity measurement area. The samples were kept in the oven during the thermal conductivity measurements with a Hot Disk device (NF EN ISO 22007-2), a transient method using a flat probe that serves both as a heating device and a temperature sensor. The probe is placed between two identical, smooth, flat samples to avoid contact with air. This measurement method allows the determination of thermal conductivity and heat capacity for any temperature, with a fast and reliable procedure. Please note that specific heat capacity values were calculated by dividing the ρc_p obtained from the Hot Disk by the density of samples assessed at each tested temperature. The Kapton 5501 probe with a radius of 6.403 mm, a power of 90 mW and a measurement time of 80 s was used for the measurement of CEB thermal conductivity. The Kapton 8563 probe with a radius of 9.868 mm was used both for LH and SB samples, with a measurement time of 80s and a power of 33mW for LH and 30mW for SB.

2.2.2 Procedure for assessing walls thermal performance

The wall samples described in paragraph 2.1 were tested inside a Thermo3 equipment, a double-room climatic chamber by 3R company. This equipment is a hot guarded box used to test full-scale walls. It is composed by two separates room, a cold and a hot room, which are thermally insulated from external effects by two guarded control zones. During a test, the difference in temperature between the two rooms create a unidirectional heat flow which cross the walls to be tested. Figure 2 shows a schema of the machine.

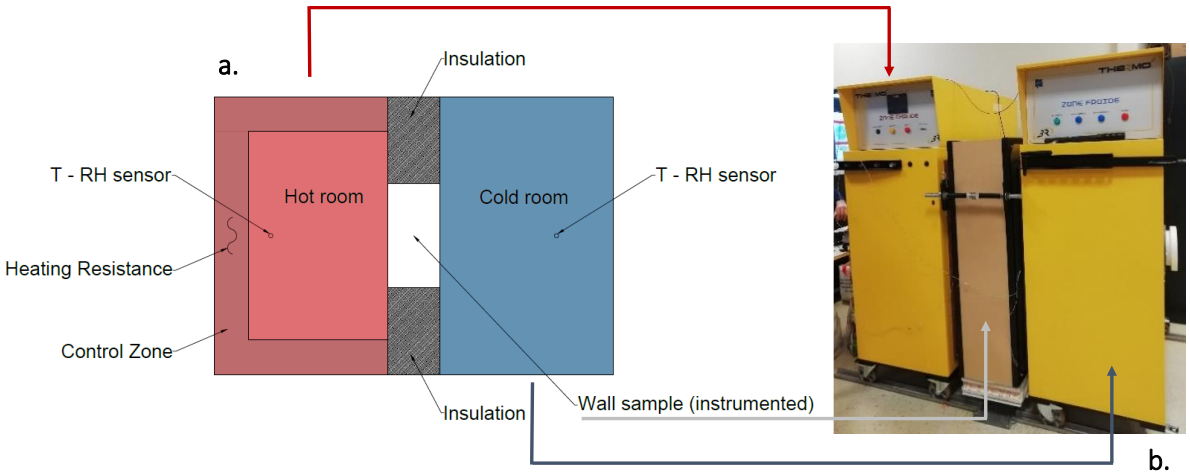

Figure 2. Schematic plan of the double room climatic chamber (a) and double room climatic chamber with testing frame (b)

In the hot room, the temperature is regulated by two heating resistances (200 W for zone) supplied at low voltage (48 VDC), located in the outer hot guarded zone. The resistances are activated each time that heat is lost from the hot to the cold room, and the amount of energy released is registered and then averaged in order to assess the heat flow through the wall. It is important to remark that the hot room is not equipped with a refrigerator system, fact which means that the temperature can never decreased, but only be increased. The range of admissible temperatures of the hot room goes from 20°C to 50°C.

The cold room is equipped with a refrigeration unit 450 W, with a cold exchanger connected to the cold zone and a hot exchanger connected to the outside. The cold room is able to increase and decrease its temperature setpoints, allowing the setting of temperature cycles. The range of admissible temperatures of the cold room goes from -20°C to 30°C.

The three wall samples are subjected to two types of tests, simulating both summer and winter seasons. In terms of winter behavior, the walls are tested under dynamic condition by using the Thermo3 option “Daily cycle”. This option allows the setting of a constant temperature in the hot room and of a sinusoidal cycle (entirely described by a maximum and a minimum temperature value and a period) on the cold room. In this test, a constant temperature of 25°C is maintained in the hot room, while the cold room’s temperatures vary between 5°C and 10°C with a 24 hours’ period. A scheme of the winter dynamic testing conditions is shown in figure 3.

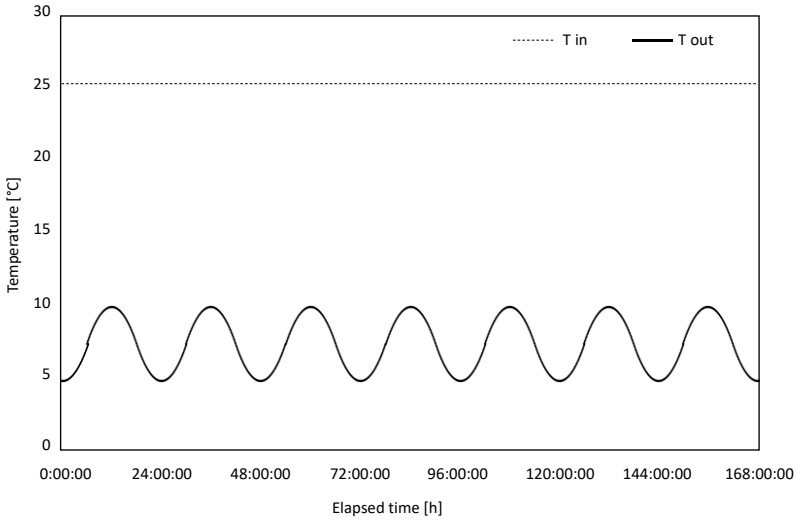

Figure 3. Winter dynamic testing conditions

The propagation of temperature profiles on the wall exposed to a variable outdoor air temperature is assumed to be sinusoidal. In the passage from outdoor to indoor surface of the wall, the amplitude of the sinusoidal temperature wave is reduced [22]. In order to quantify the thermal mass of the wall assemblies, Time lag (TL) and Decrement Factor (DF) dynamic parameters are assessed. Time lag is defined as the time interval required for the thermal wave to pass from the outer surface to the inner surface of the wall. It can be expressed by the formula:

$$TL = t_{T_{so,max}} - t_{T_{si,max}}$$

Where *t* is the time at which the peaks of indoor ($T_{si,max}$) and outdoor ($T_{so,max}$) surface temperatures occur. Time lag is expressed in hours.
The decrement factor is the ratio between the amplitude of inner surface temperatures and the amplitude of outer surface temperatures, and can be calculated as follows:

$$DF = \frac{T_{si,max} - T_{si,min}}{T_{so,max} - T_{so,min}}$$

Moreover, in the same weather and wall configuration (winter behavior, CEB wall with an exterior layer of thermal insulation), the wall is tested under static condition in order to assess its thermal resistance when the hot room temperature is 25°C, and the cold room temperatures are T=5°C and T=10°C.
Due to the limitations of the cold room in admissible temperatures range and to the absence of a refrigeration unit on the hot room which could enable the decrease of the temperature, the summer behavior cannot be assessed in dynamic conditions, so it has been estimated in static conditions. In particular, three thermal resistance measures have been performed, by maintaining the indoor temperature constant at 25°C, and by increasing the outdoor temperature at T=30°C, T=35°C and T=40°C. Due to the limitation in admissible temperatures in the cold room, the position of wall is inversed compared to the winter behavior, so in the summer tests the indoor is simulated by the cold room and the outdoor is simulated by the hot room of the equipment.
The assessment of thermal resistance is done by the formula:

$$R = \frac{T_{s,hot} - T_{s,cold}}{\varphi}$$

Where $T_{s,hot}$ is the surface temperature on the hot side of the wall, $T_{s,cold}$ is the surface temperature on the cold side of the wall, φ is the heat flow measured in W/m^2. A scheme of both winter and summer static testing conditions is shown in figure 4.

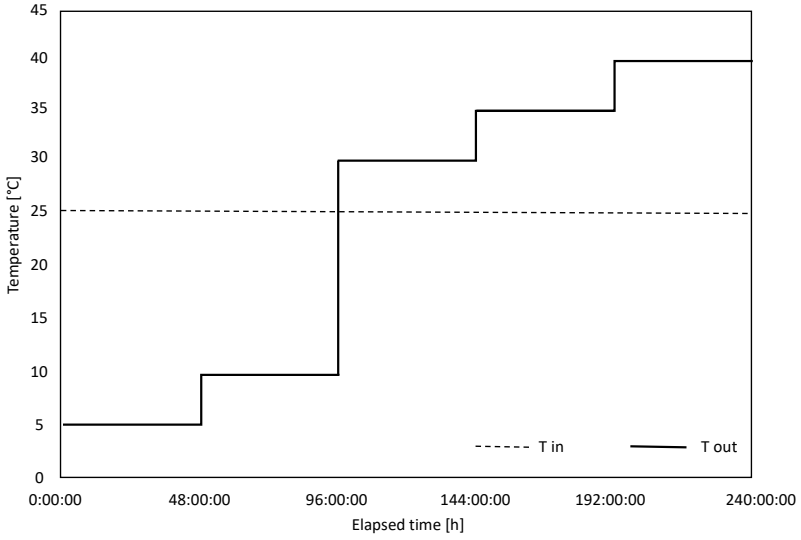

Figure 4. Static testing conditions

The positions and the types of instrumentations are reported in the following figure 5 and 6. The sensibilities of the sensors are shown in table 1.

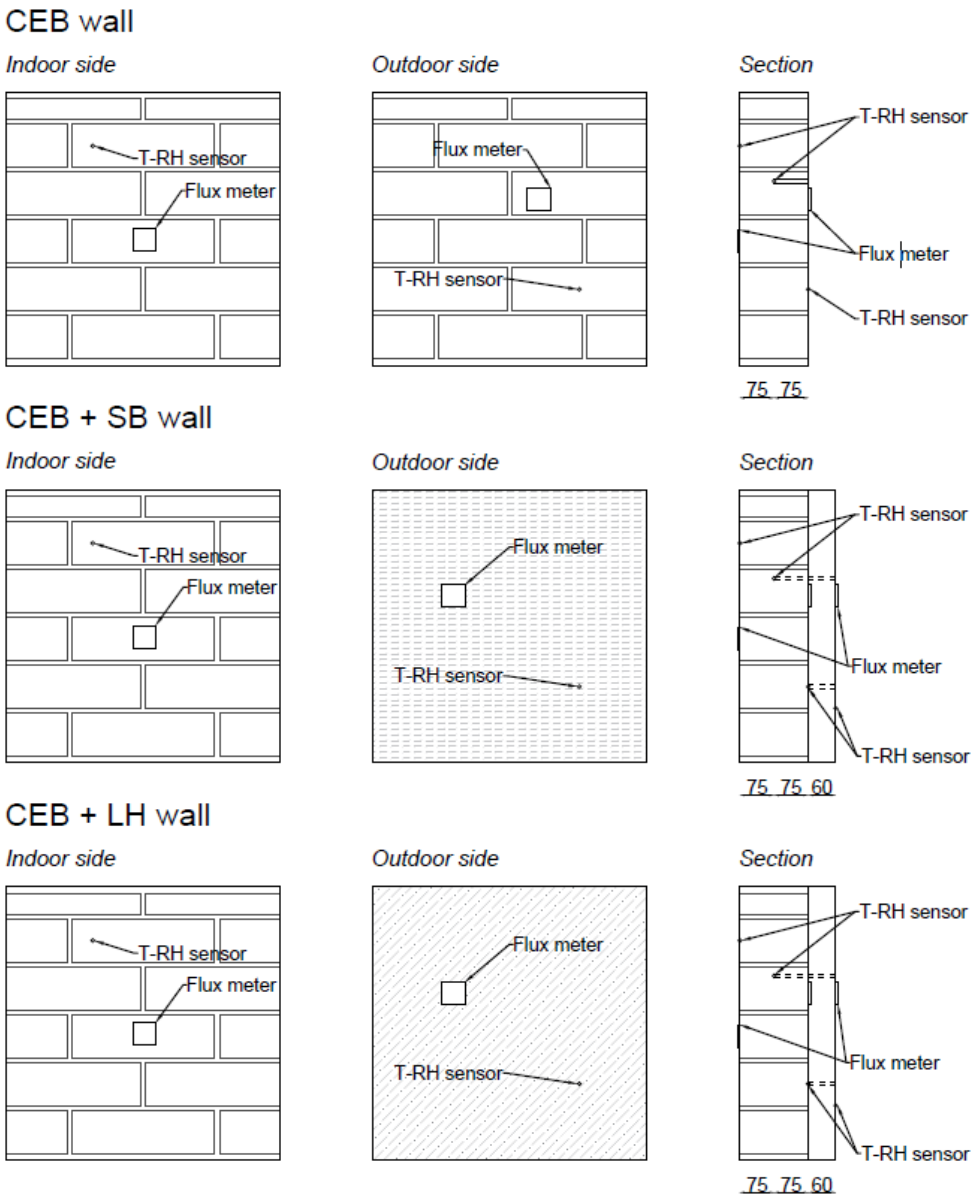

Figure 5. Wall instrumentation scheme

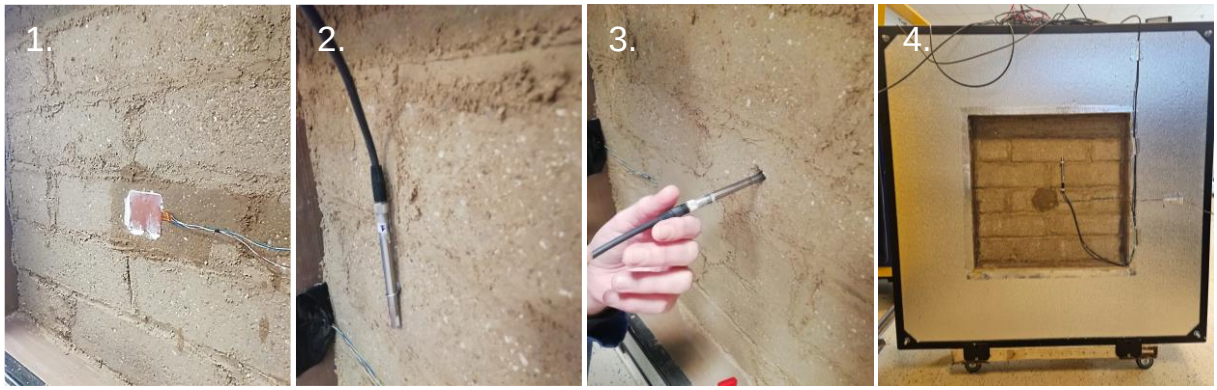

Figure 6. Instrumentation of CEB walls: installation of heat flow meter (1), T-RH sensors (2, 3), final refinements (4)

Table 1. Type and position of sensors used

Wall	Type of Sensor	Position
BTC	Heat Flow meter Captec 22.9 μV/W^{-1}m^{-2}	Indoor surface
	Heat Flow meter Captec 22.9 μV/W^{-1}m^{-2}	Outdoor surface
	3 T-RH sensors DKRF400	Indoor surface
		0.075 m deep inside the wall
		Outdoor surface
BTC + SB	Heat Flow meter Captec 22.9 μV/W^{-1}m^{-2}	Indoor surface
	Heat Flow meter Captec 22.9 μV/W^{-1}m^{-2}	Interface between CEB wall and insulation
	Heat Flow meter Captec 66.3 μV/W^{-1}m^{-2}	Outdoor surface
	4 T-RH sensors DKRF400	Indoor surface
		0.075 m deep inside the wall
		Interface between CEB wall and insulation
		Outdoor surface
BTC + LH	Heat Flow meter Captec 15.2 μV/W^{-1}m^{-2}	Indoor surface
	Heat Flow meter Captec 22.6 μV/W^{-1}m^{-2}	Interface between CEB wall and insulation
	Heat Flow meter Captec 60.0 μV/W^{-1}m^{-2}	Outdoor surface
	4 T-RH sensors DKRF400	Indoor surface
		0.075 m deep inside the wall
		Interface between CEB wall and insulation
		Outdoor surface

A resume of the wall configurations, and of static and dynamic test conditions is reported in table 2.

Table 2. Tested conditions in the Hot Guarded Box

WALL CONFIGURATION	STATIC CONDITIONS		DYNAMIC CONDITIONS
CEB	Winter conditions T_{in} 25°C T_{out} = 5°C, 10°C	Summer conditions Tin 25°C T_{out} = 30°C, 35°C, 40°C	Winter conditions T_{in} 25°C T_{out} cyclic [5;10] T=24h
CEB + SB	Winter conditions T_{in} 25°C T_{out} = 5°C, 10°C	Summer conditions Tin 25°C T_{out} = 30°C, 35°C, 40°C	Winter conditions T_{in} 25°C T_{out} cyclic [5;10] T=24h
CEB + LH	Winter conditions T_{in} 25°C T_{out} = 5°C, 10°C	Summer conditions Tin 25°C T_{out} = 30°C, 35°C, 40°C	Winter conditions T_{in} 25°C T_{out} cyclic [5;10] T=24h

3. Results and discussion

3.1 Material properties

The material properties assessed in this study have been reported in the following tables. In particular, the dry density of compressed earth blocks, sugarcane bagasse and lime hemp are reported in table 3.

Table 3. Dry density of the analyzed materials

	CEB	SB	LH
Dry density [kg/m^3]	1800±3	55±2	395±8

Figure 7 reports the values of thermal conductivity measures made on the analyzed samples as temperature varies between 25°C and 40°C. Observing the results, it is evident that all the insulating

materials as SB and LH show little variation of thermal conductivity as the temperature increase. Indeed, SB thermal conductivity is constant to 0.06 W/mK when temperature increase from 25°C to 40°C, while LH thermal conductivity ranges from 0.11 W/mK when T=25°C to 0.13 W/mK when T=40°C. Conversely, massive materials as CEB have a slightly higher thermal conductivity variation: their thermal conductivity passes from 0.83 W/mK when T=25°C to 0.86 W/mK when T=40°C. We can therefore conclude that no significant variation in thermal conductivity is observed with varying temperatures.

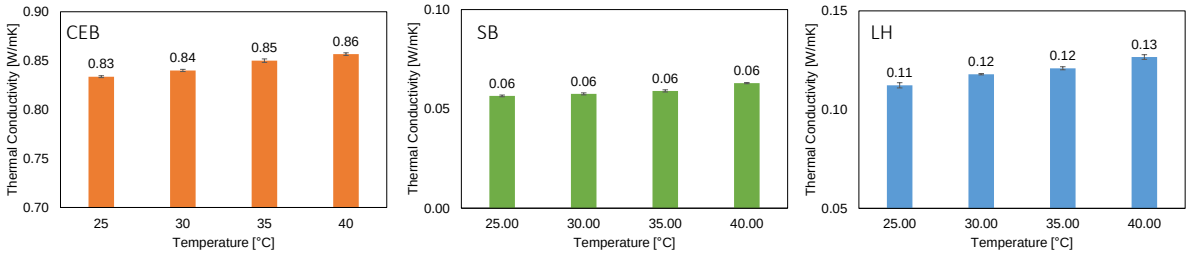

Figure 7. Temperature dependent thermal conductivity of the analyzed materials

We will now focus on figure 8. Specific heat capacity values were calculated by dividing the ρc_p obtained from the Hot Disk by the density of samples at each temperature. It was observed a reduction of dry density of samples for increasing testing temperature, fact which could be explained by the loss of some residual moisture contained inside the samples. The c_p of CEB samples varies from 713±15 J/kg K to 804±26 J/kg K for temperatures raising from 25°C to 40°C. For SB samples, they range from 2121±4 J/kg K to 2545±4 J/kg K and for LH samples from 501±9 J/kg K to 538±10 J/kg K, when temperature is increased from 25°C to 40°C.

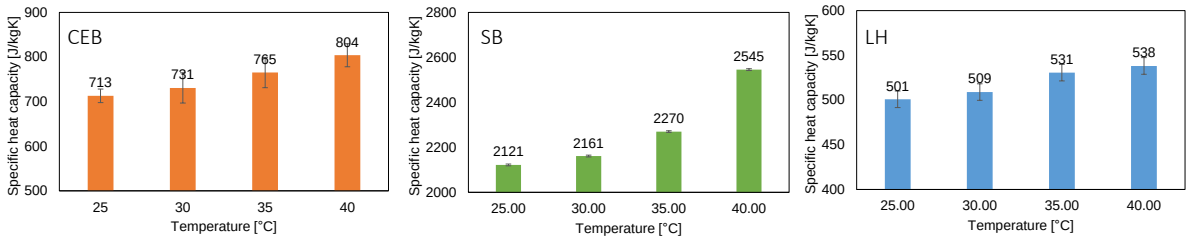

Figure 8. Temperature dependent specific heat capacity of the analyzed materials

3.2 Walls thermal performances

3.2.1 Static conditions

As anticipated in section 2.2.2, the three investigated walls were tested under several stationary conditions. In particular, indoor temperature was set to 25°C, while the outdoor one simulated both winter (T_{out} = 5°C, T_{out} = 10°C) and summer conditions (T_{out} = 30°C, T_{out} = 35°C, T_{out} = 40°C). In particular, the abovementioned outdoor air temperatures for summer conditions were chosen to allow a comparison between the R-values assessed by the Hot Guarded Box equipment and the R-values calculated from the hot disk measurements at a material scale.

Throughout the tests, heat flow entering φ_{in} and leaving φ_{out} the walls were monitored by means of the heat flow meters installed on the inmost and outmost faces of the wall, and steady-state condition was deemed to be attained when the two flows were constant across the wall for at least 24 hours. During the test, it was observed that a time interval of at least 48 hours for the walls was enough to achieve the steady-state condition.

Figure 9 shows the heat flow values calculated in the last 24 hours of the test for all the investigated wall configurations. Please note that in the calculation of the R-value, only the heat flow entering in the wall (φ_{in}) was considered, to avoid the phenomenon of thermal diffusion [24].

By observing the plotted values in figure 9, it is possible to remark that heat flow values for CEB wall are more scattered compared to those of CEB+SB wall and CEB+LH wall. Furthermore, heat flow in the insulated solutions is much lower and near for all the tested temperature conditions. In particular, for the CEB wall, in the T_{out}=5°C condition the φ_{in} is 47.55 W/m^2, in the T_{out}=10°C condition the φ_{in} is 35.74

W/m^2, in the T_{out}=30°C condition the φ_{in} is 13.08 W/m^2, in the T_{out}=35°C condition the φ_{in} is 24.59 W/m^2 and in the T_{out}=40°C condition the φ_{in} is 37.63 W/m^2. Indeed, the lower the temperature difference between indoor and outdoor, the lower the heat flow across the wall; besides, it is possible to affirm that the measured heat flows are quite high, due to the relatively high thermal conductivity of compressed earth blocks.

For the CEB+SB wall, in the T_{out}=5°C condition the φ_{in} is 12.92 W/m^2, in the T_{out}=10°C condition the φ_{in} is 9.51 W/m^2, in the T_{out}=30°C condition the φ_{in} is 3.17 W/m^2, in the T_{out}=35°C condition the φ_{in} is 5.78 W/m^2 and in the T_{out}=40°C condition the φ_{in} is 8.53 W/m^2. By comparing these heat flow values to the ones of the uninsulated CEB wall it is easy to remark the benefic effect of thermal insulation in decreasing the heat exchange between the indoor and the outdoor.

For the CEB+LH wall in winter static conditions, for the T_{out}=5°C condition the φ_{in} is 20.59 W/m^2, while for the T_{out}=10°C condition the φ_{in} is 16.15 W/m^2. Instead, in summer static conditions, for the T_{out}=30°C condition the φ_{in} is 6.83 W/m^2, for the T_{out}=35°C condition the φ_{in} is 12.44 W/m^2 and for the T_{out}=40°C condition the φ_{in} is 17.58 W/m^2. These heat flow values are less than half the heat flows for the corresponding conditions in the uninsulated CEB wall configuration, but they are in general more than double the heat flows in the CEB+SB wall configuration.

It is also possible to observe that between all the tested conditions there is a global decrease in the heat flow, with a minimum around T=25°C followed by an increase (see figure 9a). In figure 9b the measured heat flow values are plot against the absolute value of the differences between T_{in} and T_{out}.

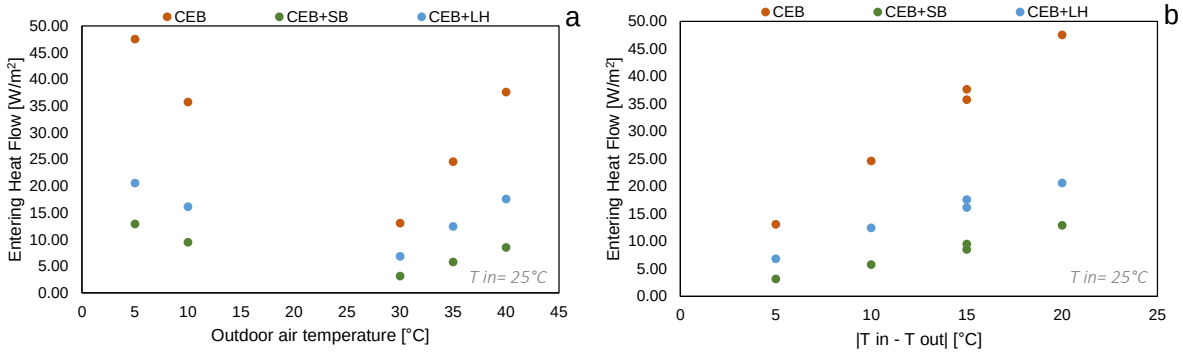

Figure 9. Heat flow entering into the wall for CEB, CEB+SB and CEB+LH wall configurations plotted against outdoor air temperature (a) and against the absolute value of the difference between indoor and outdoor air temperature (b)

Figure 10 shows the wall surface temperatures evolution for each wall and tested temperature condition. In the graph are reported both indoor (T_{si}) and outdoor (T_{so}) surface temperatures. Differently from [5], who, analyzing the behavior of several uninsulated unfired earth walls, observed the strong dependency of wall temperatures to the imposed environmental conditions, in our study the indoor surface temperature values between different wall configurations are quite scattered (as it is shown in figure 11a and 11b).

Indeed, for the CEB wall, the T_{si} = 20°C when T_{out}=5°C, T_{si} = 20.8°C when T_{out}=10°C and T_{si} ranges from 27.0 °C to 30.2 °C when T_{out} goes from 30°C to 40°C.

Instead, for the CEB+SB wall, the indoor surface temperatures between all the tested conditions are more similar between them, as they are mitigated by the insulation layer. In particular, they range from T_{si} = 23.7°C when T_{out}=5°C to T_{si} = 26.3 °C when T_{out}=40°C. Finally, for the CEB+LH wall, the indoor surface temperatures range from T_{si} = 22.1 °C when T_{out}=5°C to T_{si} = 27.1 °C when T_{out}=40°C.

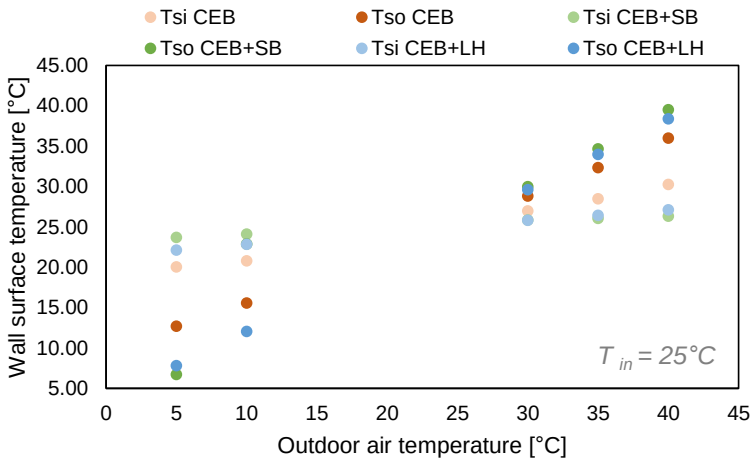

Figure 10. Wall surface temperatures in static conditions for CEB, CEB+SB and CEB+LH wall configurations (indoor air temperature T = 25 °C)

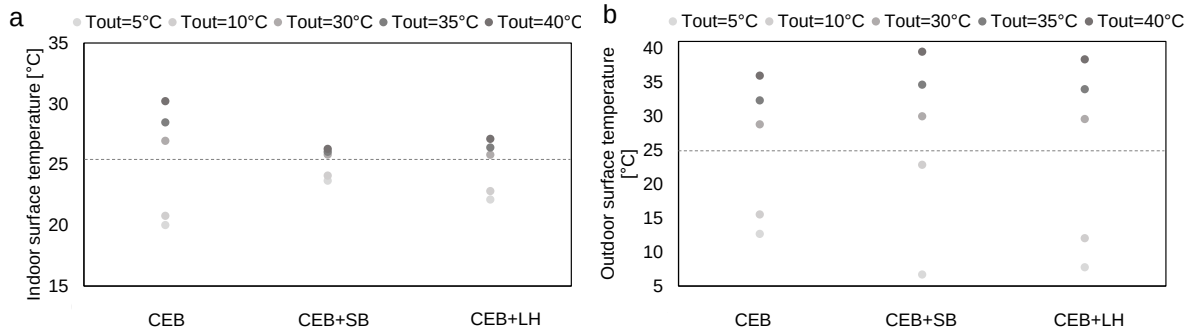

Figure 11. Effect of thermal insulation on indoor surface temperature (a) and outdoor surface temperature (b)

As explained in section 2.2.2, the heat flow and the surface temperatures measured inside the Hot Guarded Box equipment allowed, in steady-state conditions, for the assessment of the thermal resistance for all the examined walls. Thermal resistance values are reported in figure 12. For the CEB wall, the assessed thermal resistance varies between 0.14 m^2K/W and 0.16 m^2K/W for the different imposed temperature conditions. For the CEB+SB wall the thermal resistance ranges from 1.31 m^2K/W to 1.55 m^2K/W. Finally, for the CEB+LH wall the thermal resistance fluctuates between 0.55 m^2K/W and 0.70 m^2K/W. We notice that the maximum of thermal resistance in the CEB wall configuration is found in the T_{out}=35°C condition; for the CEB+SB wall configuration in the T_{out}=40°C condition, and for the CEB+LH wall configuration in the T_{out}=5°C condition.

In this study, it seemed to be interesting to compare the measured thermal resistance values to those which can be calculated from the thermal conductivity values reported in section 2.2.1. It is important to remember that in this work thermal conductivity measurements were made by means of a Hot Disk Equipment at different temperatures (ranging from 25°C to 40°C with differences of 5°C), but thermal conductivity was not assessed in correspondence of T=5°C, T=10°C due to setup limitations. For these conditions the calculated thermal resistance relies on thermal conductivity values measured at 25°C. For all the other conditions (respectively those using T_{out}=30°C, 35°C, 40 °C), the calculated thermal resistance value is evaluated by considering an average thermal conductivity between the indoor side and the outdoor side of each material used in each wall configuration. So, for instance for the static condition T_{in}=25°C and T_{out}=35°C of CEB wall, the calculated thermal resistance is an average between the R calculated with $\lambda_{25°C}$ (temperature condition on the inmost side of the wall) and the one calculated with $\lambda_{35°C}$ (temperature condition on the outmost side of the wall). It is possible to make this assumption because the surface temperatures are near to the nominative air temperatures of the two chambers. The same principle is adopted for the two CEB insulated wall solutions.

Measured (R_m) and calculated (R_c) values of thermal resistance for all the wall configurations are reported in table 4 and plotted in figure 12. Comparing the two set of values, we can observe that the

calculated values (R_c) are higher than the measured values (R_m) for the CEB wall configuration and for the CEB+LH wall configuration, while for the CEB+SB wall configuration the opposite condition occurs. If we calculate the difference between measured and calculated thermal resistances in the three test conditions, it is possible to observe that for the CEB wall, it is around 0.03 m^2K/W, for the CEB+SB wall it is on average 0.19 m^2K/W, and for the CEB+LH wall is on average 0.06 m^2K/W. This fact reveals that the CEB wall configuration is the one having the best fitting between the measured and the calculated thermal resistance values, followed by the CEB+LH wall configuration. The CEB+SB wall configuration has the highest gap between calculated and measured values of thermal resistance.

The difference between calculated and measured thermal resistance values can have several explanations. First of all, calculated values are based on the Hot disk measurements, which rely on a small depth of the material (below 1 cm), while the thermal resistance measured in the HGB involve the full thickness of CEBs and insulations. In this sense, eventual inhomogeneities of the CEBs and insulation materials might not be reflected in the λ-values calculated via the Hot disk, but would influence the R-value assessment at the wall scale.

Furthermore, in this work the influence of the laying earth mortar has not been considered as its percentage on the surface of the tested wall is fairly lower than the surface occupied by the CEBs (in particular, the surface occupied by the mortar is the 7.4% of the total surface). Nevertheless, the quantification of the contribution of the mortar layers is an aspect that should be addressed in future works.

Moreover, the gap between calculated and measured values could be due to the particular humidity conditions during the test (which were not controlled due to setup limitations).

Finally, an explanation for the higher gap between R_c and R_m values found for CEB+SB wall configuration (in particular for higher outdoor air temperature conditions) may be found in the possible presence of air leaks in the test setup, influencing the assessment of R_m. In particular some residual air resistance could be located at the interface between the sugarcane bagasse panel and the compressed earth block wall.

Table 4. Measured and calculated thermal resistance values for different outdoor air temperature

T_{out} [°C]	CEB		CEB+SB		CEB+LH	
	$R_{measured}$ [m^2K/W]	$R_{calculated}$ [m^2K/W]	$R_{measured}$ [m^2K/W]	$R_{calculated}$ [m^2K/W]	$R_{measured}$ [m^2K/W]	$R_{calculated}$ [m^2K/W]
5	0.15±0.01	0.18	1.31±0.07	1.23	0.70±0.04	0.72
10	0.15±0.01	0.18	1.34±0.03	1.23	0.67±0.05	0.72
30	0.14±0.02	0.18	1.31±0.15	1.22	0.55±0.07	0.70
35	0.16±0.02	0.18	1.49±0.12	1.20	0.61±0.05	0.68
40	0.15±0.01	0.18	1.55±0.10	1.16	0.64±0.04	0.66

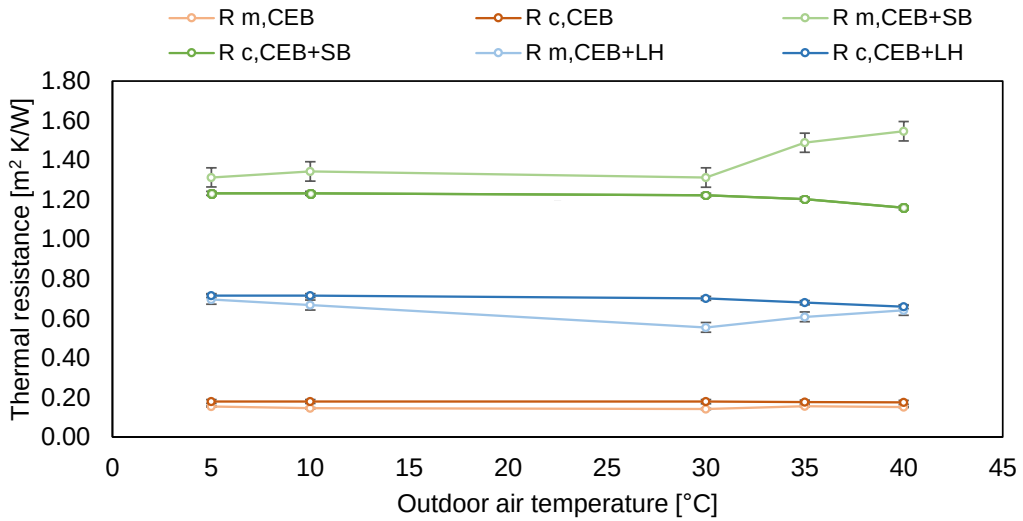

Figure 12. Measured and calculated thermal resistance of CEB, CEB+SB and CEB+LH wall configurations

3.2.2 Dynamic conditions

Under winter conditions, a dynamic test, reproducing a daily cyclic oscillation between 5°C and 10°C, is performed on the three tested wall configurations. Figure 13 reports the heat flow across the three walls under 7-days of test. In this work, the presence of wall insulation radically changes wall's behavior. The phases of the heat flow for the CEB+SB and CEB+LH walls are delayed with respect to the one of the CEB wall. The intensity of heat flow for the CEB wall is quite high, and oscillating between 41.5 W/m^2 and 35.06 W/m^2. If we now compare the behavior of the two insulated solution, the lowest heat flow is the one guaranteed by the CEB+SB wall solution, with heat flow values oscillating between 12.95 W/m^2 and 9.03 W/m^2. The CEB+LH wall has heat flow values which varies 18.75 W/m^2 and 16.86 W/m^2.

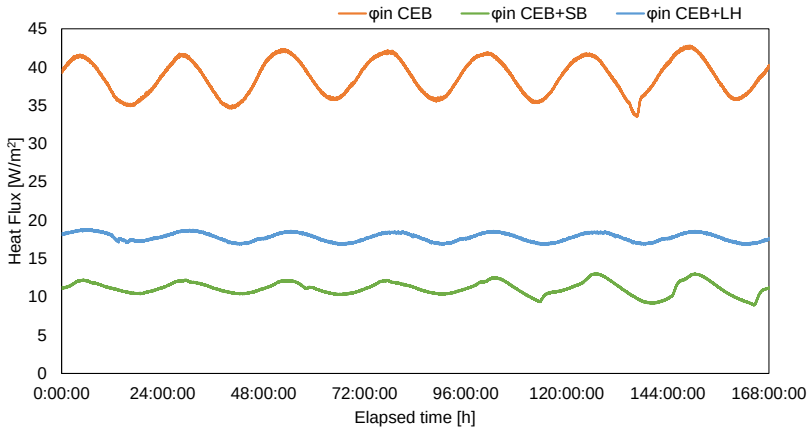

Figure 13. Heat flow across the tested walls under winter dynamic test conditions

We will now focus on the inertial behavior of the walls, and we will analyze the data which are reported in figure 14 and 15. First, when observing the indoor surface temperature values in CEB, CEB+SB and CEB+LH wall solutions, only the CEB+SB and CEB+LH solutions manage to attain values near to the indoor air temperature of 25°C. Indeed, the absence of thermal insulation in the CEB solution cause a decrease in T_{si} values, which range from 19.7 °C to 20.9 °C values which, in a living space, could have effect on the comfort of the inhabitants. This issue is exasperated by the contained thickness of the CEB wall. Conversely, CEB+SB wall have T_{si} values which range from 23.7 °C to 24.0 °C, and CEB+LH wall has temperatures which range between 22.0 °C and 22.6 °C, both nearer to comfort conditions.

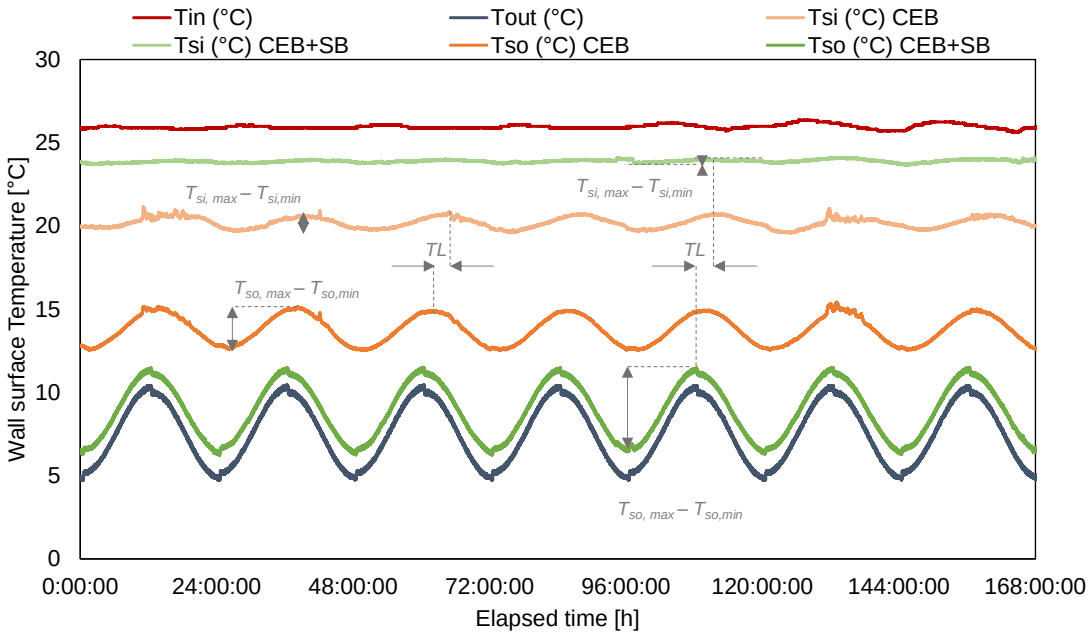

Figure 14. Daily cycle for CEB and CEB+SB wall configurations

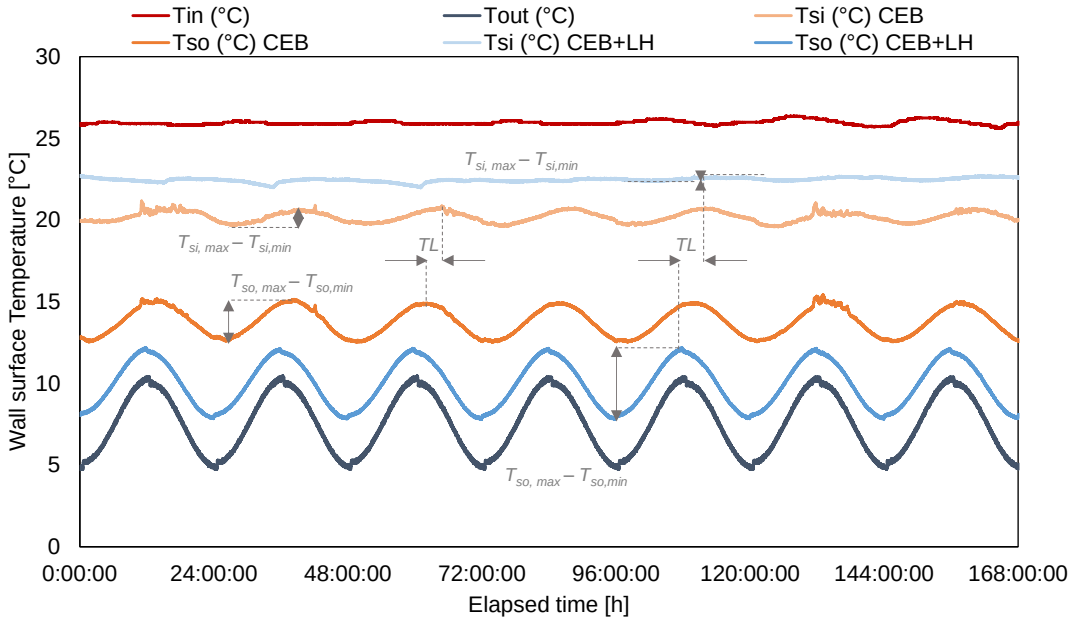

Figure 15. Daily cycle for CEB and CEB+LH wall configurations

On the base of the indoor (T_{si}) and outdoor (T_{so}) surface temperatures of the three wall configurations, and considering the time delay between the outdoor and indoor peak, it is possible to assess the time lag and decrement factor values. These parameters, which were defined in section 2.2.2, are the expression of the inertial behavior of the wall. Average results for TL and DF over 7-days of test are reported in table 5 together with other data found in the literature. It is interesting to remark the benefic effect of the thermal insulations in increasing the time lag and decreasing the decrement factor.

Table 5. Time lag and decrement factor for all the tested wall configurations and comparison with literature values

Type of wall	Reference	Average TL [h]	Average DF [-]
Hypercompacted brick (0.10 m)	[5]	1.43	0.40
Fired brick (0.11 m)	[5]	1.50	0.28
Hemp brick (0.10 m)	[5]	2.00	0.45
Uninsulated RE (0.29 m)	[6]	6.50 – 9.00	0.191 – 0.256
Wood fiber (0.06 m) insulated RE (0.29 m)	[6]	8.20 – 9.80	0.030 – 0.059
Light earth (0.03 m) insulated RE (0.12 m)	[9]	3.87 – 4.07	0.530 – 0.830
CEB (0.15 m)	*This study*	3.78	0.369
CEB+SB (0.15 m + 0.06 m)	*This study*	4.80	0.049
CEB+LH (0.15 m + 0.06 m)	*This study*	6.90	0.049

Note: RE (rammed earth), CEB (compressed earth block)

In table 5 we compare the results obtained in this study to those found in the literature. In particular, note that TL and DF of [5] were calculated by the Authors from figure 10 of [5]. For a 0.11-m thick fired brick wall [5], the time lag is around 1.5 hours, while the decrement factor is about 0.28. At the same way, it is possible to calculate that for a 0.10-m thick hypercompacted brick wall [5], the time lag is around 1.43 hours and the decrement factor is around 0.4. In [6], the uninsulated rammed earth wall, 0.29 m thick, has a time lag ranging between 6.50 and 9.00 hours and a decrement factor comprised between 0.191 – 0.256. The use of 0.06 m thick wood fiber thermal insulation increase time lag values to 9.80 hours and decrease decrement factor values to 0.03 [6]. Finally, 0.03 m thick light earth insulated rammed earth (0.12 m thick), has a time lag ranging from 3.87 to 4.07 hours and a decrement factor comprised between 0.53 and 0.83.

Values for uninsulated raw earth walls [5, 6] are in line with results found in this study for the 0.15 m-thick CEB wall: in particular it is easy to observe that the differences on dynamic wall's parameters compared to values of [5, 6] are likely to be due to the increased wall's thickness used in present study. The results found for the bio-based insulated wall configurations [6, 9 and this study] confirm that the use of thin layers of thermal insulation can be preferable to the lightening of earth mixtures in order to

enhance the dynamic thermal parameters of the walls. Indeed, the time lag values found in this study are 4.8 hours for the CEB+SB wall and 6.9 hours for the CEB+LH wall. These values are higher than those of a wall realized by lightening the compressed earth wall with hemp fibers (the hemp brick wall in [5]) for which it is calculated a time lag of 2 hours. This is confirmed by the decrement factor value found in this study for the uninsulated solution (0.049), which is below the 0.45 value calculated from [5]. Moreover, our CEB+SEB and CEB+LH wall configurations seem to perform better than [9], both in terms of TL and DF, and have comparable values to [6] even if the thicknesses of materials used are lower.

4. Conclusion

This work focused on compressed earth blocks (CEB) walls characterization at a material and at wall scale. The analyzed CEB wall configurations included an uninsulated 0.15 m thick CEB wall, and two bio-based insulated walls, one using 0.06 m-thick sugarcane bagasse insulation (CEB+SB wall) and the other using 0.06 m-thick lime hemp wall insulation (CEB+LH wall).

Materials used in this study were characterized concerning their dry density, and temperature dependent thermal conductivity and specific heat capacity were assessed by means of a Hot Disk equipment. In particular, thermal properties were assessed at 25°C, 30°C, 35°C and 40°C.

Full-scale wall's thermal behavior was studied in a Hot Guarded Box equipment, which allowed for the testing of both static and dynamic thermal conditions. The three wall configurations were tested under winter dynamic conditions (by setting an indoor air temperature of 25°C, and a varying sinusoidal outdoor air temperature between 5°C and 10°C), from which were calculated two dynamic thermal parameters, time lag and decrement factor. Moreover, five sets of static tests were performed on the three walls, by maintaining an indoor air temperature of 25°C and increasing outdoor air temperature from 5°C, to 10°C, 30°C, 35°C and 40°C. The measures of surface temperatures and heat flows from the static tests were used to measure the thermal resistance on site. Finally, the thermal resistance values measured on site for each outdoor temperature condition were compared to the thermal resistances calculated from thermal conductivity values assessed at the material scale.

Results on walls' thermal resistance show that there is a slight difference between R-value calculated from the thermal conductivity assessments done at a material scale and R-value calculated on full-scale walls. In particular, this study finds out that for CEB and CEB+LH wall configurations, calculated R-values are higher than measured R-values, while for CEB+SB wall the opposite condition occurs, and measured R-values are higher than calculated R-values for all the tested temperatures. This can be explained by the presence of some residual air layer between the sugarcane bagasse panel and the compressed earth blocks walls in the tested setup, or by a competing effect of relative humidity.

In general, thermal resistance of weakly bio-based insulated CEB walls are found to be nine times (for the CEB+SB wall) and four times (for the CEB+LH wall) higher than that of uninsulated CEB wall.

The dynamic test conditions allowed for the estimation of indoor surface temperatures (T_{si}) for a wide series of outdoor air temperatures. For the CEB wall, T_{si} range from 19.7 °C to 20.9 °C. For the CEB+SB wall, T_{si} range from 23.7 °C to 24.0 °C, and for CEB+LH wall temperatures range between 22.0°C and 23.0 °C.

Dynamic thermal parameters found in this study confirm the optimal potentialities of CEB walls to guarantee comfortable indoor conditions. For a 0.15 m-thick CEB wall the time lag is 3.78 hours, while for the CEB+SB wall is 4.8 hours and for the CEB+LH wall is 6.9 hours. Besides, the decrement factor of CEB wall is 0.369, while for both the bio-based insulated CEB walls is 0.049.

Future studies will have to focus on the influence that different relative humidity conditions (determined for example by different vapor concentration classes depending on the intended use of the building) can have on the static and dynamic behavior of CEB walls. In this sense, the choice of combining bio-based thermal insulations with CEBs will be additionally scrutinized through the lens of material compatibility from a hygrometric point of view. In addition, the behavior of uninsulated and bio-based insulated CEB walls should be tested in cyclic hygrothermal conditions, in order to estimate the effect of the hygrothermal fatigue on these materials. Finally, the execution of cyclic tests in climate-controlled chambers, which could reproduce the real operating conditions of full-scale earthen walls, including the effect of rain and solar radiation, would allow predicting the seasonal behavior of the walls and the durability of these technological solutions over time.

CRediT authorship contribution statement

Giada Giuffrida: Writing- Original draft preparation, Visualization, Investigation, Software, Data curation, Conceptualization, Methodology. **Laurent Ibos:** Writing- Reviewing and Editing, Investigation, Software, Data curation, Supervision, Resources, Validation, Conceptualization, Methodology. **Abderrahim Boudenne:** Writing- Reviewing and Editing, Resources, Validation, Conceptualization, Methodology. **Hamza Allam:** Writing- Reviewing and Editing, Validation, Supervision, Project administration, Conceptualization, Methodology.

Acknowledgements

The authors want to acknowledge *Cycle Terre* and *Emerwall* Companies for the interest in the research and the continuous technical exchange.

References

1. SRIA 2023, ECTP Strategic Research & Innovation Agenda 2021-2027
2. De Luca G., Coppola O., Franco A., Bonati A., 2023, Double "CE" for Construction Products: "Circular Economy" in "CE Marking", Civil Eng Res J 13(5)
3. Bender A.P., Bilotta P., 2019, Circular Economy and Urban Mining: Resource Efficiency in the Construction Sector for Sustainable Cities, In: Leal Filho, W., Azul, A., Brandli, L., Özuyar, P., Wall, T. (eds) Sustainable Cities and Communities. Encyclopedia of the UN Sustainable Development Goals. Springer, Cham. https://doi.org/10.1007/978-3-319-71061-7_40-1
4. Mellado Mascaraque M.A., Castilla Pacual F.J., Oteiza I., Aparicio Secanellas S., 2020, Hygrothermal assessment of a traditional earthen wall in a dry Mediterranean climate, Building Research & Information, 48:6, 632-644, DOI: 10.1080/09613218.2019.1709787
5. Bruno AW, Gallipoli D, Perlot C, Kallel H, Thermal performance of fired and unfired earth bricks walls, Journal of Building Engineering 28 (2020) 101017
6. Serrano S., De Gracia A., Cabeza L.F., 2016, Adaptation of rammed earth to modern construction systems: Comparative study of thermal behavior under summer conditions, Applied Energy (175), 180-188
7. Goodhew S, Boutouil M, Streiff F, Le Guern M, Carfrae J, Fox M, Improving the thermal performance of earthen walls to satisfy current building regulations, Energy & Buildings 240 (2021) 110873
8. Jimenez C., Wieser M., Biondi S., 2017, Improving thermal performance of traditional cabins in the high-altitude Peruvian Andean Region, Proceedings of the PLEA 2017 Conference – Design to Thrive
9. Pennacchio R., Piccablotto G., 2017, Rammed earth buildings to meet Italian thermal regulation: monitoring and sample tests, in: Mileto C., Vegas Lopez-Manzanares F., Garcia Sorano L., Cristini V. (Eds.) Vernacular and Earthen Architecture: Conservation and Sustainability, SosTierra 2017, Valencia, Spain, 14-16 September 2017)
10. Grazieschi G., Asdrubali F., Thomas G., 2021, Embodied energy and carbon of building insulating materials: A critical review, Cleaner Environmental Systems 2,100032
11. Füchsl S., Rheude F., Röder H., 2022, Life cycle assessment (LCA) of thermal insulation materials: A critical review, Cleaner Materials (5), 100119
12. Fiche technique Bloc BTC Cycle Terre: https://www.cycle-terre.eu/wp-content/uploads/2021/04/FT_BTC_201108.pdf
13. Turco C, P. Junior Ad, Teixeira ER, Mateus R, Optimisation of Compressed Earth Blocks (CEBs) using natural origin materials: A systematic literature review, Construction and Building Materials 309 (2021) 125140
14. Lamrani M, Mansour M, Laaroussi N, Khalfaoui M, Thermal study of clay bricks reinforced by three ecological materials in south of morocco, Energy Procedia, 156, 2019, 273-277
15. Oti JE, Kinuthia JM, Bai J, Design thermal values for unfired clay bricks, Materials and Design, 31(1), 2010, 104 - 112
16. Poullain P, Leklou N, Laibi AB, Gomina M, Properties of Compressed Earth Blocks Made of Traditional Materials from Benin, Revue de Composites et des Materiaux Avancés, 29(4), 2019, 233 – 241
17. Ben Mansour M, Jelidi A, Cherif AS, Jabrallah SB, Optimizing thermal and mechanical performance of compressed earth blocks (CEB), Construction and Building Materials, 104, 2016, 44-51
18. Jami T, Karade SR, Singh LP, A review of the properties of hemp concrete for green building applications, Journal of Cleaner Production 239 (2019) 117852

19. Collet, F., 2017. Hygric and thermal properties of bio-aggregate based building materials. In: Amziane, S., Collet, F. (Eds.), Bio-aggregates Based Building Materials: State-Of-The-Art Report of the RILEM Technical Committee 236-BBM. Springer Netherlands, Dordrecht, pp. 125 - 147.
20. Ramlee NA, Naveen J, Jawaid M, Potential of oil palm empty fruit bunch (OPEFB) and sugarcane bagassefibers for thermal insulation application – A review, Construction and Building Materials 271 (2021) 121519;
21. Mehrzad S, Taban E, Soltani P, Samaei SE, Khavanin A, Sugarcane bagasse waste fibers as novel thermal insulation and sound-absorbing materials for application in sustainable buildings, Building and Environment 211 (2022) 108753
22. Giuffrida G, Detommaso M, Nocera F, Caponetto R. Design Optimisation Strategies for Solid Rammed Earth Walls in Mediterranean Climates. Energies. 2021; 14(2):325.
23. Neya I, Yamegueu D, Coulibaly Y, Messan A, Ouedraogo ALSN, Impact of insulation and wall thickness in compressed earth buildings in hot and dry tropical regions, Journal of Building Engineering, 33, 2021, 101612
24. François A., Ibos L., Feuillet V., Meulemans J., 2020, Novel *in situ* measurement methods of the total heat transfer coefficient on building walls, Energy & Buildings 219,110004